10th International Electronic Conference on Synthetic Organic Chemistry (ECSOC-10). 1-30 November 2006. http://www.usc.es/congresos/ecsoc/10/ECSOC10.htm & http://www.mdpi.org/ecsoc-10/

[g004]

Modeling of acetylene pyrolysis under vacuum carburizing conditions of steel in a tubular flow reactor

R.U.Khan * , S.Bajohr, F.Graf, R.Reimert

Engler Bunte Institute,University of Karlsruhe,76131-Karlsruhe Germany

Abstract

In the present work, the pyrolysis of acetylene was studied under the conditions of vacuum carburizing of steel in a tubular flow reactor. The pyrolysis temperature ranges from 650 ^{o}C to 1050 ^{o}C . The partial pressure of acetylene in the feed mixture was 10 mbar and 20 mbar respectively while the rest of the mixture consisted of nitrogen. The total pressure of the mixture was 1.6 bar. A kinetic mechanism which consists of 7 species and 9 reactions has been used in the commercial CFD code Fluent. Species transport and reaction model of Fluent was used in the simulations. The comparison of simulations and experimental results is presented in this paper.

Key words: Acetylene, Pyrolysis, Modeling, Simulation, Carburizing

1 Introduction

Amongst the many applications of acetylene, carburizing of steel is upcoming. The pyrolysis of acetylene has been studied by many researchers under various conditions depending upon its application considered. Detailed kinetic mechanisms proposed in literature consist of hundreds of species and reactions. Typically, these investigations include shock tube pyrolysis of acetylene[1–12] and pyrolysis in flow systems[13–15]. The deposition of pyrolytic carbon from various hydrocarbons has also been described by some researchers[16–20]. Although the detailed kinetic mechanisms are considered to be more accurate and reliable, their use is mostly limited to ideal flow models. Use of such detailed kinetic mechanisms is not easy with transport models in CFD codes

* Corresponding author.
Email address: *rafi_ullah.khan@ciw.uni-karlsruhe.de* (R.U.Khan).

with present computational hardware and algorithms. However CFD codes normally implement Navier-Stokes equations to model transport and are used for modeling flow field even when the geometry is complex. Operational kinetic mechanisms or reduced versions of detailed mechanisms can be used with CFD codes for modeling the reacting flow. The vacuum carburizing with acetylene involves the pyrolysis of acetylene under very low pressure which produces solid carbon along with other hydrocarbon gases making the flow field more complex. Diffusion of carbon into the surface of steel takes place which is continued until the desired carbon content and case depth is achieved. In the present work, the pyrolysis of acetylene was studied under the conditions of vacuum carburizing of steel.

2 Results and Discussions

The measured products of pyrolysis which include solid carbon, CH_4, C_2H_2, C_2H_4, C_4H_4, C_6H_6 have been reported as percentage of input feed carbon content at different temperatures. The experimental results are compared with the simulation results of Fluent version 6.2. The amount of hydrogen was calculated by material balance and is also compared with the simulation results.

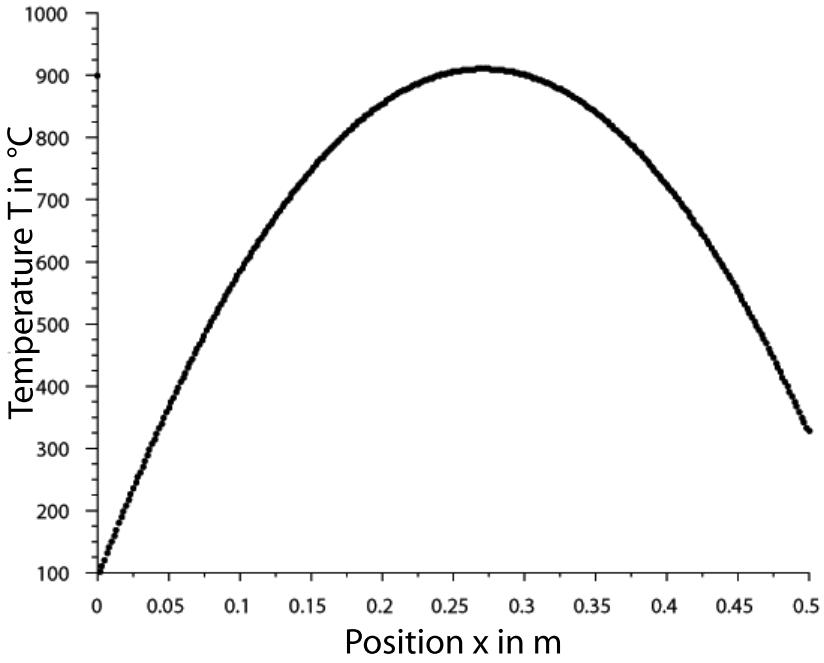

Fig. 1. Temperature profile at a controller temperature T_c of 900 ^{o}C

Fig. 2. Contours of mole fraction of C_2H_2 at 900 ^{o}C and 20 mbar partial pressure of acetylene

Fig. 3. Contours of mole fraction of $C_{(s)}$ at 900 ^{o}C and 20 mbar partial pressure of acetylene

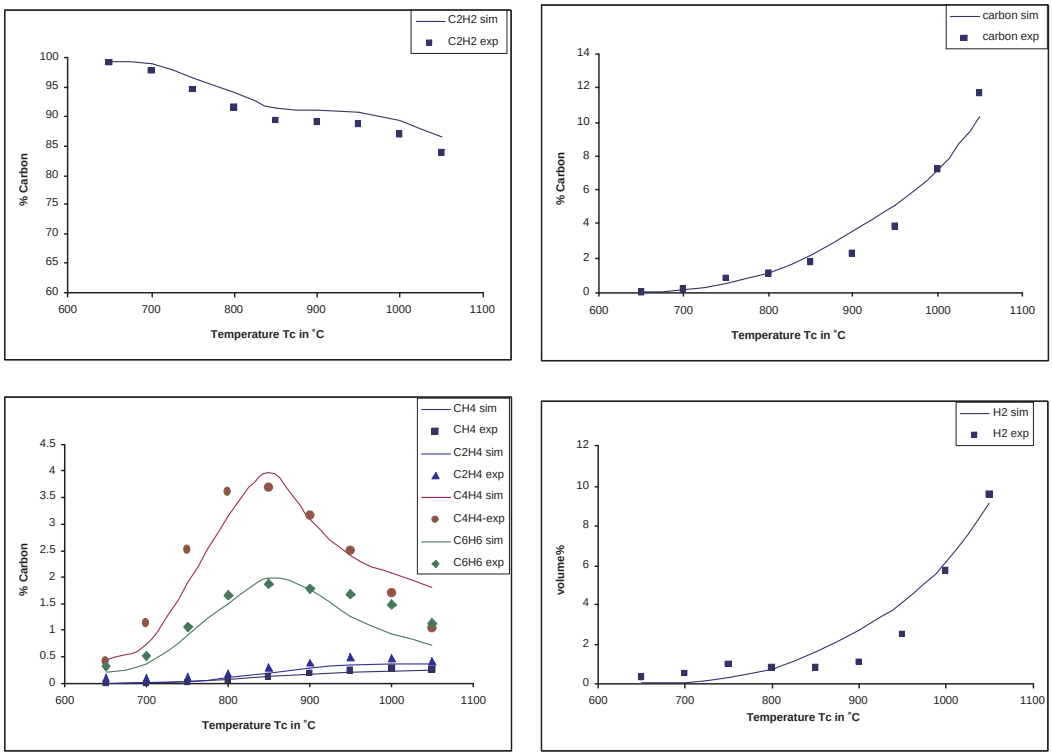

Fig. 4. Comparison of simulated vs experimental results at 10 mbar acetylene partial pressure

Fig. 2 and Fig. 3 represent two of the typical contours of mole fractions obtained from simulations for two important species C_2H_2 and $C_{(s)}$ at 900 ^{o}C and 20 mbar partial pressure of acetylene. Fig. 4 shows the comparison of experimental and simulation results for acetylene at 10 mbar partial pressure for a controller temperature variation of 650 ^{o}C to 1050 ^{o}C. The carbon content carried by unconverted acetylene in the mixture decreases from 99 % at 650 ^{o}C to 75 % at 1050 ^{o}C for 20 mbar representing a conversion of 25 % of acetylene to other products at the outlet as shown in Fig. 5. The second major and important component carrying carbon among the pyrolysis products is the solid carbon for which results are shown for 10 mbar as well as for 20 mbar partial pressure of acetylene. The percentage of solid carbon increases with an increase in temperature. The formation of C_4H_4 and C_6H_6 increases up to a temperature of 900 ^{o}C and then gradually decreases at higher temperatures.

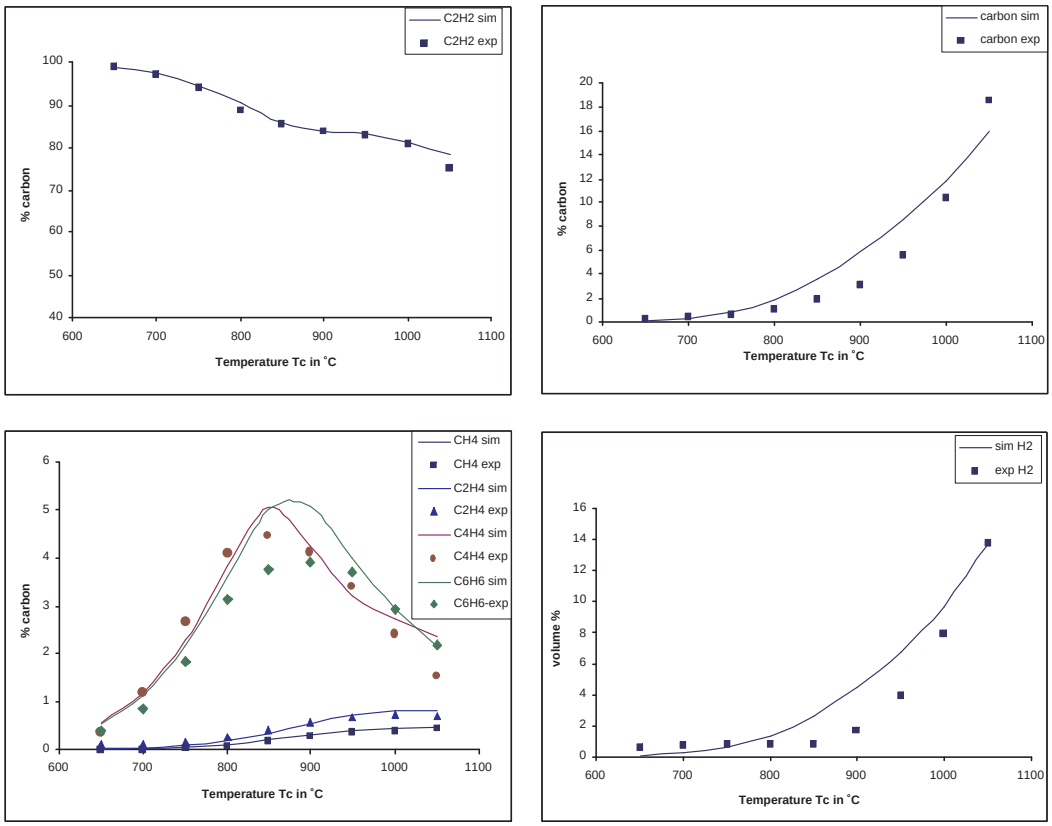

Fig. 5. Comparison of simulated vs experimental results at 20 mbar acetylene partial pressure

CH_4 and C_2H_4 are also formed but the carbon content in these compounds is less than 1 % under these experimental conditions.

3 Reaction Mechanism and CFD Model

The reaction mechanism shown in table 1 consists of 7 species which are the major products of acetylene pyrolysis under the vacuum carburizing conditions of steel. These include solid carbon $C_{(s)}$ and hydrocarbons consisting of $CH_4, C_2H_2, C_2H_4, C_4H_4, C_6H_6$ along with H_2. The overall mechanism consists of 9 reactions. The estimated Arrhenius parameters, activation energies and proposed reaction rates are also shown in the table 1. A 2-D grid consisting of 300 x 20 cells has been used to represent a reactor length of 500 mm with diameter of 20 mm. The species transport and reaction model in Fluent was used for modeling the chemistry. The mechanism discussed above was implemented through a user defined function (UDF) in Fluent. The operating pressure was set equal to 1.6 bar while inlet temperature and velocity boundary conditions were used according to the experimental measurements. As the

Table 1
Proposed reaction mechanism of acetylene pyrolysis

rate constant $k_i = A_i e^{-E_i/RT}$				
Nr	Reaction	Rate Expression	$A_i(mol, m^3, s)$	E_i(kJ/mol)
1	$C_2H_2 + H_2 \rightarrow C_2H_4$	$r_1 = k_1.c_{C_2H_2}.c_{H_2}^{0.36}$	$4.4 \cdot 10^3$	103.0
2	$C_2H_4 \rightarrow C_2H_2 + H_2$	$r_2 = k_2.c_{C_2H_4}^{0.5}$	$3.8 \cdot 10^7$	200.0
3	$C_2H_2 + 3H_2 \rightarrow 2CH_4$	$r_3 = k_3.c_{C_2H_2}^{0.35}.c_{H_2}^{0.22}$	$1.4 \cdot 10^5$	150.0
4	$2CH_4 \rightarrow C_2H_2 + 3H_2$	$r_4 = k_4.c_{CH_4}^{0.21}$	$8.6 \cdot 10^6$	195.0
5	$C_2H_2 \rightarrow 2C_{(s)} + H_2$	$r_5 = k_5.\frac{c_{C_2H_2}^{1.9}}{1+18c_{H_2}}$	$5.5 \cdot 10^6$	165.0
6	$C_2H_2 + C_2H_2 \rightarrow C_4H_4$	$r_6 = k_6.c_{C_2H_2}^{1.6}$	$1.2 \cdot 10^5$	120.7
7	$C_4H_4 \rightarrow C_2H_2 + C_2H_2$	$r_7 = k_7.c_{C_4H_4}^{0.75}$	$1.0 \cdot 10^{15}$	335.2
8	$C_4H_4 + C_2H_2 \rightarrow C_6H_6$	$r_8 = k_8.c_{C_2H_2}^{1.3}.c_{C_4H_4}^{0.6}$	$1.8 \cdot 10^3$	64.5
9	$C_6H_6 \rightarrow 6C_{(s)} + 3H_2$	$r_9 = k_9.\frac{c_{C_6H_6}^{0.75}}{1+22c_{H_2}}$	$1.0 \cdot 10^3$	75.0

reactor is not operated under isothermal conditions, a temperature profile was necessary to model the temperature field. A mathematical fit in the form of a polynomial shown in equation (1) below was used for the temperature profile in the simulations.

$$T(x) = (a \cdot x^2 + b \cdot x + c) \cdot T_c + d \cdot x^2 + e \cdot x + f \tag{1}$$

T(x) represents the temperature as a function of the position x in relation to the reactor length. T_c represents controller temperature. This temperature profile was also implemented through a user defined function (UDF) and compiled before loading into Fluent using the default procedures in Fluent. A typical temperature profile implemented in Fluent is shown in Fig. 1. The solution was converged to species residuals of 10^{-6} or less so that there was no further variation of these residuals. The convergence was fast and achieved in less than 500 iterations.

4 Experimental

A ceramic reactor with an inner diameter of 20 mm, outer diameter of 25 mm and a length of 600 mm was used in the present investigations. At the outlet of the reactor is a ceramic filter which can separate entrained solid carbon from the gas stream. The products of pyrolysis in the gas phase were measured by gas chromatography. The temperature profile was measured at the center of the reactor in an interior ceramic pipe with an outer diameter of 6 mm.

5 Conclusion

Acetylene pyrolysis has been modeled by using simplified chemistry with a transport model under the particular conditions of the industrial process of vacuum carburizing of steel. Comparison of simulated and experimental results show satisfactory agreement under technical operating conditions. Further investigations for complex geometries are necessary to prove the validity of the model for the application as a prediction tool to control the carburizing process in commercial plants.

References

[1] C.H. Wu, H.J. Singh, and R.D. Kern. Pyrolysis of acetylene behind reflected shock waves. *International Journal of Chemical Kinetics*, 19(11):975–996, 1987.

[2] M. Frenklach, M.B. Durgaprasad, S. Taki, and R. Matula. Soot formation in shock-tube pyrolysis of acetylene, allene, and 1, 3-butadiene. *Combustion and Flame*, 54:81–101, 1983.

[3] M. Frenklach, D.W. Clary, W.C. Gardiner, and S.E. Stein. Detailed kinetic modeling of soot formation in shock-tube pyrolysis of acetylene. *Proc. Combust. Inst*, 20:887–901, 1984.

[4] M. Frenklach. Reaction mechanism of soot formation in flames. *Physical Chemistry Chemical Physics*, 4(11):2028–2037, 2002.

[5] M.H. Back. Mechanism of the Pyrolysis of Acetylene. *Canadian Journal of Chemistry*, 49(13):2199–2204, 1971.

[6] J.H. Kiefer, W.A. Von Drasek, and W.A. Von Drasek. The mechanism of the homogeneous pyrolysis of acetylene. *International Journal of Chemical Kinetics*, 22(7):747–786, 1990.

[7] I. D. Gay, G. B. Kistiakowsky, J. V. Michael, and H. Niki. Thermal decomposition of acetylene in shock waves. *The Journal of Chemical Physics*, 2004.

[8] T. Kruse and P. Roth. Kinetics of C_2 Reactions during High-Temperature Pyrolysis of Acetylene. *Journal of Physical Chemistry A*, 101:2138–2146, 1997.

[9] T. Tanzawa and W.C. Gardiner, Jr. Reaction mechanism of the homogeneous thermal decomposition of acetylene. *The Journal of Physical Chemistry*, 84(3):236–239, 1980.

[10] A. Laskin and H. Wang. On initiation reactions of acetylene oxidation in shock tubes-a quantum mechanical and kinetic modeling study. *Chemical Physics Letters*, 303(1):43–49, 1999.

[11] J.H. Kiefer, S.S. Sidhu, R.D. Kern, K. Xie, H. Chen, and L.B. Harding. The homogeneous pyrolysis of acetylene II: the high temperature radical chain mechanism. *Combustion science and technology*, 82(1-6):101–130, 1992.

[12] H. Böhm and H. Jander. PAH formation in acetylene-benzene pyrolysis. *PCCP. Physical chemistry chemical physics(Print)*, 1(16):3775–3781, 1999.

[13] K. Norinaga, O. Deutschmann, and K. J. Huttinger. Analysis of gas phase compounds in chemical vapor deposition of carbon from light hydrocarbons. *Carbon*, 44:1790–1800, 2006.

[14] S.T. Dimitrijevic, S. Paterson, and P.D. Pacey. Pyrolysis of acetylene during viscous flow at low conversions; influence of acetone. *Journal of Analytical and Applied Pyrolysis*, 53(1):107–122, 2000.

[15] C. F. Cullis and N. H. Franklin. The pyrolysis of mixtures of acetylene with other hydrocarbons. *Combustion and Flame*, 8:246–248, 1964.

[16] A.V. Krestinin. On the Kinetics of Heterogeneous Acetylene Pyrolysis. *Kinetics and Catalysis*, 41(6):729–736, 2000.

[17] Z. J. Hu and K. J. Huttinger. Mechanisms of carbon deposition-a kinetic approach. *Carbon*, 40:624–628, 2002.

[18] Z. J. Hu and K. J. Huttinger. Influence of the surface area/volume ratio on the chemistry of carbon deposition from methane. *Carbon*, 41:1501–1508, 2003.

[19] K. Norinaga and K.J. Huttinger. Kinetics of surface reactions in carbon deposition from light hydrocarbons. *Carbon*, 41(8):1509–1514, 2003.

[20] W.G. Zhang, Z.J. Hu, and K.J. Huttinger. Chemical vapor infiltration of carbon fiber felt: optimization of densification and carbon microstructure. *Carbon*, 40(14):2529–2545, 2002.